Clinical and Translational Imaging
https://doi.org/10.1007/s40336-024-00626-3

ORIGINAL ARTICLE

Assessment of diffuse bone marrow involvement on 18F-fluoro-D-glucose PET/computed tomography

Tong Zhang[1] · Lei Wang[1] · Funing Yang[2] · Hongjia Wang[2] · Ping Li[2]

Received: 7 October 2023 / Accepted: 9 February 2024

Abstract

Purpose This study aims to investigate the role of bone marrow (BM) FDG uptake distribution in assessing pathological status of BM with diffusely increased FDG uptake.

Methods We retrospectively analyzed one hundred and thirty-four PET/CT scans with diffusely hypermetabolic BM, which involved forty-nine patients with BM malignant infiltration (BMI) and eighty-five patients with benign BM disorders. The maximum standardized uptake values (SUVmax) of axial skeletons, appendicular skeletons, and the range of humerus FDG uptake were measured. The clinical and laboratory data were collected. Multivariate logistic regression analysis and receiver operating characteristic (ROC) curve were used to evaluate the risk factors for BMI and discriminative ability of above indicators for the pathology status of BM.

Results In patients with diffusely hypermetabolic BM, both the glucose metabolism of axial and appendicular skeletons was higher in BMI than BM benign disorders. The multivariate logistic regression analysis (stepwise) revealed age (odds ratio [OR] 1.073; 95%CI, 1.031–1.117; $P=0.001$), femurs SUVmax (OR 2.058; 95%CI, 1.317–3.218; $P=0.002$), neutrophil count (OR 0.805; 95%CI, 0.718–0.902; $P<0.001$) and range of humerus FDG uptake (OR 11.335; 95%CI, 2.831–45.377; $P=0.001$) were associated with BMI. Combined diagnosis had the highest ROC value (AUC 0.918; 95%CI, 0.864–0.973; $P<0.001$) with a sensitivity of 89.8% and specificity of 85.9%.

Conclusion The BM activity of the appendicular skeleton was more significant in distinguishing BM malignant and benign disorders. Range of humerus FDG uptake combined femurs SUVmax, neutrophil count and age was reliable for assessing diffuse BM involvement.

Keywords Bone marrow · ^{18}F-FDG PET/CT · Hematopoietic malignancies · Autoimmune diseases

Introduction

As a major hematopoietic organ, bone marrow (BM) is a critical site for the production, differentiation, and maturation of blood cells. Actively hematopoietic BM is characteristically located in the central cavities of axial and long bones in adults [1]. The evaluation of BM is a routine procedure in hematopoietic diseases, and the bone marrow aspiration/biopsy (BMA/BMB) is commonly used to determine the pathological status of BM [2].

^{18}F-fluorodeoxyglucose (^{18}F-FDG) is an analogue of glucose, which is used in positron emission tomography/computed tomography (PET/CT) and generally accumulates in the hypermetabolic cells. BM FDG uptake is helpful to examine the function of red marrow and to detect BM involvement in both benign and malignant disorders. The obvious advantages of evaluating BM diseases using FDG PET/CT include the capacity of quantifying the glucose metabolism, whole-body imaging, and noninvasive examination [2, 3]. Physiological FDG accumulation throughout the skeletons is associated with the hematopoietic activity and is compatible with the normal distribution of hematopoietic marrow [4, 5]. BM is generally defined as

✉ Ping Li
lipinghmu@163.com

Tong Zhang
zt1393209748@163.com

[1] Department of Nuclear Medicine, Jilin Cancer Hospital, Changchun, China

[2] Department of Nuclear Medicine, the Second Affiliated Hospital of Harbin Medical University, Baojian Road, Nangang District, Harbin, Heilongjiang Province, China

Published online: 04 March 2024

"hypermetabolic" if its FDG avidity exceeds that in the liver [6]. However, FDG is not specific to malignancies, accumulated FDG in BM may indicate active hematopoiesis [7, 8]. Diffusely hypermetabolic BM may appear in not only BM malignant infiltration (BMI) but also BM benign disorders [3], posing a diagnostic challenge for identifying BM pathological status correctly.

Accurate assessment of hypermetabolic BM on FDG PET/CT is helpful to avoid unnecessary BMA/BMB and guide subsequent treatment. Limited findings suggested that FDG uptake in spine BM was higher in BMI than non-BMI diseases [9]. Super BM uptake defined as the spine BM maximum standardized uptake values (SUVmax) similar to or higher than the brain SUVmax was a highly potent indicator for BMI [10]. Although the spine FDG uptake seemed helpful to distinguish malignant and benign BM involvement, its diagnostic value was limited because of the high specificity and low sensitivity [9, 10], still leaving a gray zone of diagnostic indetermination. In addition, few studies evaluated the association between the BM activity of appendicular skeleton and BMI. In this study, we compared the FDG uptake of axial and appendicular skeletons in malignant and benign BM involvement, explore the risk factors for BMI and assessed the discriminative ability of FDG PET/CT, clinical and laboratory parameters for BM pathological status.

Materials and methods

Patients

The BMA reports, medical records, and FDG PET/CT examinations of patients who underwent FDG PET/CT at our hospital from September 2017 to March 2023 were reviewed. The inclusion criteria include: (i) patients with diffusely increased BM FDG uptake; (ii) patients underwent BMA examination within one week of FDG PET/CT examination; (iii) patients with a definite diagnosis. The exclusion criteria include: (i) patients administered hematopoietic cytokines therapy before 10 days of FDG PET/CT examination; (ii) patients with pathological bone destruction. This retrospective study was approved by the Human Research Protection Office (HRPO) at our institution. Patient informed consent was waived.

Clinical and laboratory data collection

Clinical data included age, sex, glucose level, and with a fever or not. Laboratory data included white blood cell (WBC), neutrophil, lymphocyte, monocyte, and platelet counts, and hemoglobin, which all were measured within one week of the FDG PET/CT examination.

FDG PET/CT image acquisition

FDG PET/CT images were acquired with a PET/CT system (Biograph 64 mCT, Siemens Healthcare, Erlangen, Germany) combining a full-ring PET scanner. Patients fasted for 6 h before intravenous injection of ^{18}F-FDG (4.07 MBq/kg, 0.11 mCi/kg). Blood glucose levels of all patients were less than 11 mmol/L before the procedure. ^{18}F-FDG with a minimum radiochemical purity of 98% was provided. PET images were generated at one site using a similar protocol. Three-dimensional (3D) emission and transmission scanning were acquired from the base of the skull to the mid-femur approximately 60 min after FDG injection. Ture D fusion was carried out and PET images were reconstructed with a slice thickness of 1 mm.

Assessment of FDG PET/CT scans

Semi-quantitative analysis of the FDG metabolism was quantified by the SUVmax. The SUVmax in axial skeletons (spine, ribs, sternum, pelvis), appendicular skeletons (proximal humerus, proximal femur, clavicle, scapula), liver and spleen were measured. The range of FDG uptake in humerus was observed and recorded as level 0 to level 3, which represented no FDG uptake, less than 1/3 uptake, 1/3 to 2/3 uptake, and more than 2/3 uptake respectively. Spine SUVmax was obtained separately from cervical vertebra 4 to cervical vertebra 7 and thoracic vertebra 8 to lumbar vertebra 5 then averaged (except for compression fractures, severe osteoarthritis changes, or lesions). Pelvis SUVmax was measured by manually drawing the outline on the central level of the second sacral vertebra. Liver and spleen SUVmax were obtained respectively by drawing three spherical volumes of interest (VOI) of 1.5 cm on different slices of liver and spleen, excluding large vessels and lesions, and then averaged. The rib SUVmax was measured from right and left rib 7 and averaged. Humerus and femurs SUVmax were measured at the site of proximal 1/3 humerus/femurs. The assessment was conducted blindly by Nuclear Medicine specialist who was unaware of the pathological results (Fig. 1).

Statistical analysis

All continuous variables were checked for normal distribution by Shapiro-Wilk tests. Normally distributed variables, nonnormally distributed variables, categorical variables were compared with the Student's T-test, Rank sum test and Chi-Square test respectively. Risk factors for BM

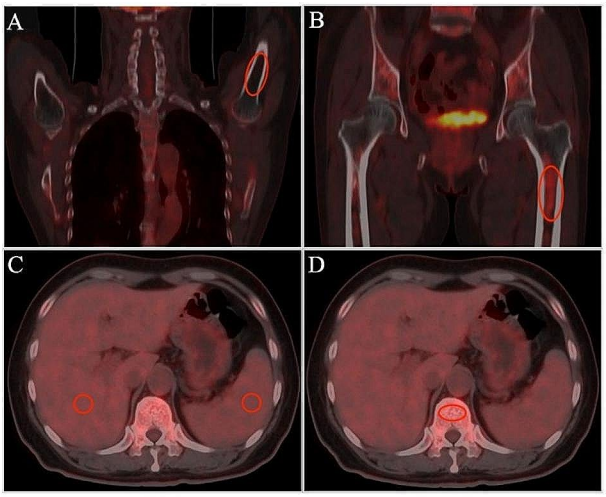

Fig. 1 The volumes of interest (VOI) used to calculate SUVmax. **A**, **B**, Humerus/femurs SUVmax was measured by drawing an elliptical VOI at the site of proximal 1/3 humerus/femurs. **C**, Liver and spleen SUVmax were obtained respectively by drawing three spherical VOI of 1.5 cm on different slices. **D**, Spine SUVmax was obtained by drawing an elliptical VOI on the center of centrum

malignancies were determined by multivariate logistic regression analysis (stepwise). The discriminative ability of FDG PET/CT, clinical and laboratory values, and combined diagnosis for BMI were evaluated using area under the receiver operating characteristic (ROC) analysis. The area under the ROC curve (AUC) was presented with 95% confidence interval (CI), and the Youden index was used to identify the maximal cut-off value. All statistical analysis were conducted using IBM Statistical Package for the Social Sciences (SPSS) version 22. P-value < 0.05 were considered statistically significant.

Results

Spectrum of BM malignant and benign diseases

forty-nine patients with BMI and eighty-five patients with BM benign disorders were enrolled in this study. The majority of BMI were diagnosed as lymphoma marrow infiltration, myeloproliferative neoplasms (MPNs), acute leukemia, Multiple Myeloma (MM), and myelodysplastic syndromes (MDS). The patients with BM benign disorders were diagnosed as autoimmune diseases, infectious diseases, lymphoma, iron-deficiency anemia (IDA) and megaloblastic anemia (Table 1).

Comparisons of FDG PET/CT, clinical and laboratory variables between BM malignant and benign diseases

The SUVmax of spine, ribs, sternum, pelvis, humerus, femur, clavicle, scapula, liver and spleen, the proportion of humerus FDG range of level 3, the proportion of man, age and platelet count in BMI were higher compared with BM benign disorders. The proportion of fever, proportion of humerus FDG range of level 0, WBC count, neutrophil count, monocyte count and hemoglobin were higher in BM benign disorders than BMI (Table 2).

Associated variables for the diagnosis of BMI

We next evaluated the risk factors for BMI in patients with diffusely hypermetabolic BM. The multivariate logistic regression analysis (stepwise) revealed age (odds ratio [OR] 1.073; 95%CI, 1.031–1.117; $P = 0.001$), femurs SUVmax (OR 2.058; 95%CI, 1.317–3.218; $P = 0.002$), neutrophil count (OR 0.805; 95%CI, 0.718–0.902; $P < 0.001$) and humerus FDG uptake of level 3 (OR 11.335; 95%CI, 2.831–45.377; $P = 0.001$) were associated with BMI (Table 3). The risk of diagnosing as BMI in level 3 group was about 11 times that of level 0 group. Finally, The −2log likelihood (-2LL) was 90.5. There was no multicollinearity among the four independent factors included in multivariate logistic regression model (Table 4).

Assessment of the discriminative ability for BMI

ROC analysis was performed to evaluate the discriminative ability of combined diagnosis and interested FDG PET/CT

Table 1 Spectrum of BM malignant and benign diseases

BMI (n = 49)		BM benign disorders (n = 85)	
Aggressive or highly aggressive lymphoma marrow infiltration	15(30.6%)	Autoimmune diseases	44(51.8%)
MPNs	15(30.6%)	Infectious diseases	21(24.7%)
Indolent lymphoma marrow infiltration	6(12.2%)	Lymphoma	14(16.5%)
Acute leukemia	5(10.2%)	IDA	5(5.9%)
MM	4(8.2%)	Megaloblastic anemia	1(1.2%)
MDS	2(4.1%)		
Hodgkin lymphoma marrow infiltration	1(2.0%)		
Bone marrow metastasis of lung cancer	1(2.0%)		

Myeloproliferative neoplasms (MPNs), Multiple Myeloma (MM), Myelodysplastic syndromes (MDS), iron-deficiency anemia (IDA).

Table 2 Comparisons of PET/CT, clinical and laboratory variables between BM malignant and benign diseases

Variables	BMI	Benign disorders	*P*-value
Age(years)	58.8 ± 12.8	47.1 ± 16.5	<0.001
Gender(man)	31(63.3%)	36(42.4%)	0.020
Glucose level(mmol/l)	5.6(5.2,6.2)	5.4(4.9,6.0)	0.058
Fever frequency	25(51.0%)	58(68.2%)	0.048
Spine SUVmax	3.49(2.91,4.55)	3.16(2.78,3.94)	0.050
Ribs SUVmax	1.99(1.66,2.62)	1.57(1.33,2.02)	<0.001
Sternum SUVmax	3.26(2.54,4.31)	2.67(2.14,3.40)	0.002
Clavicle SUVmax	1.60(1.12,2.61)	0.98(0.69,1.40)	<0.001
Scapula SUVmax	2.39(2.01,3.40)	2.01(1.62,2.42)	0.001
Pelvis SUVmax	3.87(3.00,4.71)	3.08(2.58,3.79)	0.001
Humerus SUVmax	3.12(1.65,4.01)	0.86(0.61,2.09)	<0.001
Femur SUVmax	3.50(2.70,5.22)	2.45(1.30,3.38)	<0.001
Liver SUVmax	2.50(2.06,2.95)	2.28(2.01,2.54)	0.021
Spleen SUVmax	3.22(2.55,4.53)	2.70(2.22,3.33)	0.004
Range of humerus FDG uptake			
Level 0	9(18.4%)	50(58.8%)	<0.001
Level 1	5(10.2%)	18(21.2%)	0.105
Level 2	7(14.3%)	10(11.8%)	0.673
Level 3	28(57.1%)	7(8.2%)	<0.001
WBC count($\times10^9$/L)	4.80(2.45,10.45)	9.00(5.45,13.85)	0.002
Neutrophil count($\times10^9$/L)	1.62(0.78,4.41)	6.60(3.81,11.51)	<0.001
Lymphocyte count($\times10^9$/L)	1.12(0.66,1.80)	1.31(0.94,2.01)	0.098
Monocyte count($\times10^9$/L)	0.18(0.09,0.40)	0.35(0.18,0.51)	0.008
Platelet count($\times10^9$/L)	113.0(63.0,289.0)	104.0(91.0,122.0)	<0.001
Hemoglobin(g/l)	86.0(68.0,98.0)	258.0(155.0,399.5)	<0.001

Normally distributed data, nonnormally distributed data and categorical variables were presented as mean ± standard deviation, median with interquartile range (P_{25}, P_{75}) and frequencies(percentages) respectively.

Table 3 Multivariate logistic regression analysis for BMI

Variables		B	*P*-value	OR (95%CI)
Age		0.071	0.001	1.073(1.031–1.117)
Femurs SUVmax		0.722	0.002	2.058(1.317–3.218)
Neutrophil count		-0.217	< 0.001	0.805(0.718–0.902)
Range of humerus FDG uptake	Level 0	-	0.003	-
	Level 1	-0.048	0.953	0.953(0.197–4.622)
	Level 2	0.441	0.607	1.555(0.289–8.357)
	Level 3	2.428	0.001	11.335(2.831–45.377)

Table 4 Multicollinearity analysis of multivariate logistic regression model

Model	Tolerance	VIF
Age	0.952	1.051
Range of humerus FDG uptake	0.705	1.419
Femur SUVmax	0.713	1.403
Neutrophil count	0.945	1.058

Every tolerance exceeded 0.1 and every variance inflation factor (VIF) was lower than 10, indicating there was not multicollinearity among the four factors.

variables (Fig. 2). The ROC curve revealed age combined femurs SUVmax, neutrophil count and range of humerus FDG uptake had the highest ROC value (AUC 0.918; 95%CI, 0.864–0.973; $P < 0.001$) with a sensitivity of 89.8% and specificity of 85.9%. Range of humerus FDG uptake with a cutoff value of level 2 had a sensitivity of 71.4% and specificity of 80.0% (AUC 0.795; 95%CI, 0.711–0.880; $P < 0.001$). Humerus SUVmax with a cutoff value of 2.29 had a sensitivity of 69.4% and specificity of 81.2% (AUC 0.786; 95%CI, 0.700-0.873; $P < 0.001$). Spine SUVmax showed lower ROC value (AUC 0.602; 95%CI, 0.501–0.702; $P = 0.05$).

Comparison of spine SUVmax between specific BMI and BM benign disorders

We used the spine SUVmax, which has the most BM volume, as a proxy for axial BM SUVmax. The spine

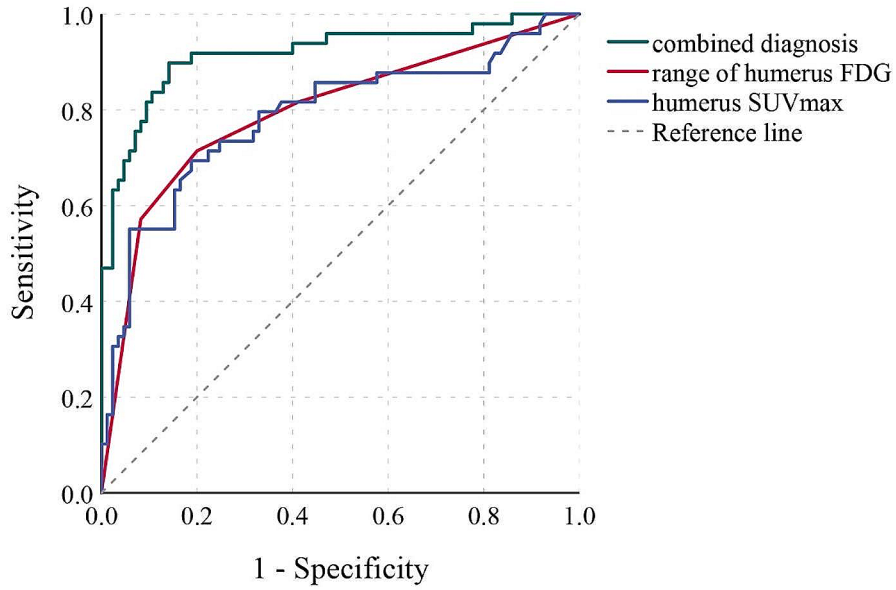

Fig. 2 The ROC curve of combined diagnosis, range of humerus FDG and humerus SUVmax. The ROC curve revealed age combined femurs SUVmax, neutrophil count and range of humerus FDG uptake had the highest ROC value (AUC 0.918; 95%CI, 0.864–0.973; $P < 0.001$)

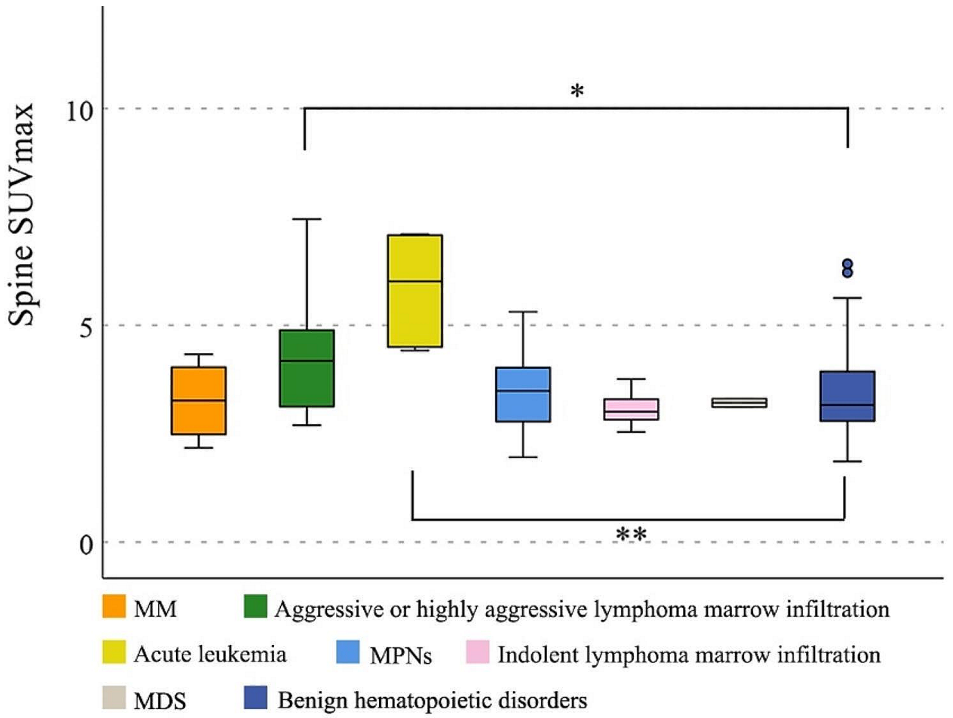

Fig. 3 The comparison of spine SUVmax between specific BMI and BM benign disorders. Spine SUVmax was significantly higher in acute leukemia and aggressive or highly aggressive lymphoma marrow infiltration than in BM benign disorders. **, $P < 0.01$; *, $P < 0.05$

SUVmax in MM, aggressive or highly aggressive lymphoma marrow infiltration, acute leukemia, MPNs, indolent lymphoma marrow infiltration, MDS and BM metastasis was 3.26(2.33,4.18), 4.18(3.09,5.07), 6.01(4.46,7.09), 3.49(2.70,4.05), 3.01(2.79,3.36), 3.11(3.21,3.21) and 12.81 respectively. Take the spine SUVmax for example, we found the axial BM FDG uptake in acute leukemia ($P = 0.001$), aggressive or highly aggressive lymphoma marrow infiltration ($P = 0.032$), BM metastasis ($P = 0.023$) was significantly higher than BM benign disorders. While there was no statistical difference between MM, MPNs, MDS, indolent lymphoma marrow infiltration and BM benign disorders (Fig. 3).

Discussion

With ageing and the change of marrow function, the pattern and amount of the FDG uptake in BM will vary. In adults, the FDG accumulation throughout the skeletons was compatible with the distribution of red marrow and characteristically located in the central cavities of axial bones, while red marrow that consists of actively hematopoietic cells was usually replaced by yellow marrow that mainly consists of adipocytes in appendicular skeletons [1, 4].

A previous study reported BMI occupied 36.8% of mildly and moderately diffuse increase in BM FDG uptake, and 93.5% of super BM uptake [10]. In this study, 49(36.3%) patients with diffusely increased FDG uptake in BM were diagnosed as BMI. Lymphoma marrow infiltration and MPNs accounted for a considerable proportion of BMI. MPNs are clonal hematopoietic disorders characterized, in chronic phase, by an overproduction of differentiated hematopoietic cells. Chronic myeloid leukemia, polycythemia vera, essential thrombocythemia, and myelofibrosis were main diseases of MPNs [11]. BM presented with significant FDG heterogeneity in BMI, which was related to the histological type of cell infiltrated. Take the spine SUVmax for example, we found that in acute leukemia, aggressive or highly aggressive lymphoma marrow infiltration were significantly higher than BM benign disorders, while spine SUVmax in MM, MPNs, MDS and indolent lymphoma marrow infiltration showed no significant difference compared to BM benign disorders. Previous study also reported the super BM FDG uptake mostly originated from acute leukemia and highly aggressive lymphoma [10]. Spine SUVmax showed lower ROC value for BMI compared to humerus SUVmax in this study. These results indicated that the FDG uptake in axial BM of some types of BMI overlapped significantly with BM benign disorders. It was unreliable to distinguish benign and malignant BM involvement only depending on the FDG uptake of axial BM.

In this study, although both the glucose metabolism of axial skeleton and appendicular skeleton was higher in BMI than BM benign disorders, the BM activity of appendicular skeletons seemed more useful at identifying BM pathological status. The range of humerus FDG uptake and humerus SUVmax showed the higher ROC value among all imaging variables. The multivariate logistic regression model showed that range of humerus FDG uptake of level 3 and higher femur SUVmax were the risk factors for BMI. Previous studies also found leukemia and MM might show greater FDG distribution in appendicular skeletons [12, 13]. This might be due to peripheral BM extension was more common in BMI [3]. The excessive growth of malignant cells exacerbated the hypoxic, acidic, and low-nutrient marrow microenvironment, destroying the survival of normal hematopoietic cells and furtherly promoting peripheral BM extension [14]. Higher SUVmax and lager metabolic range of appendicular skeletons might be new characteristics of BMI.

Increased BM FDG uptake was a sensitive marker of stimulated hematopoiesis. BM FDG uptake was closely associated with systemic inflammation and hematopoietic response caused by some tumors, infectious diseases and autoimmune diseases [15–18]. BM FDG uptake have been proven as a predictor for solid tumor progression [19]. Some studies were inclined to attribute hypermetabolic BM to active hematopoiesis of myeloid granulocytes in infectious and autoimmune diseases [20–22].

Clinical and laboratory variables also showed distinct patterns in BMI and BM benign disorders. The most valuable indicators were age and neutrophil count. Older age and lower neutrophil count were the risk factors for BMI. As steady-state hematopoiesis was switched to emergency hematopoiesis, active granulocyte progenitors generated higher neutrophil count in systemic inflammatory diseases [16–18], while neutrophil count was decreased due to the destroy of marrow architecture in BMI [3].

Given the limitations of BMA/BMB, a noninvasive technique for evaluating the hematopoietic activity and BM pathological status, would therefore be invaluable. We emphasized the BM activity in appendicular skeletons on FDG PET/CT combined clinical and laboratory variables was reliable for the assessment of diffuse BM involvement.

The limitations to our study included the nature of retrospective observational studies, which might generate the bias in patient selection and analysis. Also, routine PET/CT scans were acquired from the base of the skull to the mid-femur due to the retrospective study, so it was incapable to evaluate the FDG distribution in whole appendicular skeletons.

Conclusion

The BM activity of the appendicular skeleton was more significant in distinguishing BM malignant and benign disorders compared to axial skeleton. Range of humerus FDG uptake combined femurs SUVmax, neutrophil count and age was reliable for assessing diffuse BM involvement.

Funding/support: This study was supported by the Jilin Province Industrial Technology Research and Development Project (No.2023C040-5).

References

1. Travlos GS (2006) Normal structure, function, and histology of the bone marrow. Toxicol Pathol 34(5):548–565
2. Tomasian A, Jennings JW (2022) Bone marrow aspiration and biopsy: techniques and practice implications. Skeletal Radiol 51(1):81–88
3. Agool A, Glaudemans AW, Boersma HH et al (2011) Radionuclide imaging of bone marrow disorders. Eur J Nucl Med Mol Imaging 38(1):166–178
4. Shen G, Liang M, Su M et al (2018) Physiological uptake of 18F-FDG in the vertebral bone marrow in healthy adults on PET/CT imaging. Acta Radiol 59(12):1487–1493
5. Murata Y, Kubota K, Yukihiro M et al (2006) Correlations between 18F-FDG uptake by bone marrow and hematological parameters: measurements by PET/CT. Nucl Med Biol 33(8):999–1004
6. Inoue K, Goto R, Okada K et al (2009) A bone marrow F-18 FDG uptake exceeding the liver uptake may indicate bone marrow hyperactivity. Ann Nucl Med 23(7):643–649
7. Van Der Valk FM, Kuijk C, Verweij SL et al (2017) Increased haematopoietic activity in patients with atherosclerosis. Eur Heart J 38(6):425–432
8. Devesa A, Lobo-Gonzalez M, Martinez-Milla J et al (2022) Bone marrow activation in response to metabolic syndrome and early atherosclerosis. Eur Heart J 43(19):1809–1828
9. Zhou M, Chen Y, Liu J et al (2018) A predicting model of bone marrow malignant infiltration in (18)F-FDG PET/CT images with increased diffuse bone marrow FDG uptake. J Cancer 9(10):1737–1744
10. Alam MS, Fu L, Ren YY et al (2016) 18F-FDG super bone marrow uptake: a highly potent indicator for the malignant infiltration. Med (Baltim) 95(52):e5579
11. Nangalia J, Green AR (2017) Myeloproliferative neoplasms: from origins to outcomes. Blood 130(23):2475–2483
12. Arimoto MK, Nakamoto Y, Nakatani K et al (2015) Increased bone marrow uptake of 18F-FDG in leukemia patients: preliminary findings. Springerplus 4:521
13. Paschali A, Panagiotidis E, Triantafyllou T et al (2021) A proposed index of diffuse bone marrow [18F]-FDG uptake and PET skeletal patterns correlate with myeloma prognostic markers, plasma cell morphology, and response to therapy. Eur J Nucl Med Mol Imaging 48(5):1487–1497
14. Xu B, Hu R, Liang Z et al (2021) Metabolic regulation of the bone marrow microenvironment in leukemia. Blood Rev 48:100786
15. Patel NH, Osborne MT, Teague H et al (2021) Heightened splenic and bone marrow uptake of (18)F-FDG PET/CT is associated with systemic inflammation and subclinical atherosclerosis by CCTA in psoriasis: an observational study. Atherosclerosis 339:20–26
16. Ahn SS, Hwang SH, Jung SM et al (2017) Evaluation of spleen glucose metabolism using (18)F-FDG PET/CT in patients with Febrile Autoimmune Disease. J Nucl Med 58(3):507–513
17. Pijl JP, Kwee TC, Slart R et al (2021) Clinical implications of increased uptake in bone marrow and spleen on FDG-PET in patients with bacteremia. Eur J Nucl Med Mol Imaging 48(5):1467–1477
18. Dolan RD, Mclees NG, Irfan A et al (2019) The relationship between Tumor glucose metabolism and host systemic inflammatory responses in patients with Cancer: a systematic review. J Nucl Med 60(4):467–471
19. Jeong SY, Kim SJ, Pak K et al (2018) Prognostic value of 18F-fluorodeoxyglucose bone marrow uptake in patients with solid tumors: a meta-analysis. Med (Baltim) 97(43):e12859
20. Boursier C, Duval X, Mahida B et al (2021) Hypermetabolism of the spleen or bone marrow is an additional albeit indirect sign of infective endocarditis at FDG-PET. J Nucl Cardiol 28(6):2533–2542
21. Zhang T, Zhang J, Wang H et al (2023) Correlations between glucose metabolism of bone marrow on 18 F-fluoro-D-glucose PET/computed tomography and hematopoietic cell populations in autoimmune diseases. Nucl Med Commun 44(3):212–218
22. Ganz T (2019) Anemia of inflammation. N Engl J Med 381(12):1148–1157